

PRNU-Based detection of Morphed Face Images

K.Srinivasa Rao¹, Tammalala sai padmaja², Gurram madhavi³, Samala jyothsna⁴

¹ Assistant Professor, ^{2,3,4} B.Tech Students

ABSTRACT

Recently, researchers found that the intended generalizability of face recognition systems increases their vulnerability against attacks. In particular, the attacks based on morphed face images pose a severe security risk to face recognition systems. In the last few years, the topic of (face) image morphing and automated morphing attack detection has sparked the interest of several research laboratories working in the field of biometrics and many different approaches have been published. In this paper, a morphing attack detection system based on the analysis of "Photo Response Non Uniformity" (PRNU) is presented. More specifically, spatial and spectral features extracted from PRNU patterns across image cells are analysed and also analyses DFT plot for spatial features and absolute DFT for spectral features. This PRNU can be extracted by using DWT. Differences of these features for bona fide and morphed images are estimated during a threshold-selection at last. The proposed PRNU-based morphing attack detector is shown to robustly distinguish bona fide and morphed face images.

Keywords - Biometrics, face recognition, face morphing, face morphing attack, morphing, attack detection photo response non uniformity.

Date of Submission: 26-06-2021

Date of Acceptance: 08-07-2021

I. INTRODUCTION

Automated face recognition [1], [2] represents a longstanding field of research in which a major break-through has been achieved by the introduction of deep neural networks [3], [4]. Due to the high generalization capabilities of deep neural networks specifically and recognition systems in general, the performance of operational face recognition systems in unconstrained environments, e.g., regarding illumination, poses, image quality or cameras, improved significantly and recognition systems in general, the performance of operational face recognition systems in unconstrained environments, e.g., regarding poses, image quality or cameras, improved significantly. FACE recognition systems have recently been exposed to be vulnerable against attacks based on morphed face images [5], [6].

Image morphing has been an active field of image processing research since the 1980s [7], [8] with a variety of application scenarios, especially in the film industry. Morphing techniques can be used to create artificial biometric samples that resemble the biometric information of two (or more) individuals in the image and feature domain. In many countries, the face image used for the ePassport application process is provided by the morphed face image, he will receive a valid ePassport equipped with corresponding document security features. . It is important to note that

morphed face images can be realistic enough to fool human examiners [6], [7] as well as commercial face recognition systems. Both the criminal and the accomplice could then be successfully verified against the morphed image stored in the ePassport. This means that the criminal can use the ePassport issued to the accomplice to pass through Automated Border Control (ABC) gates (or even human inspections at border crossings). The risk of this attack, called face morphing attack, is amplified by the fact that realistic face morphs can be generated by non-experts PRNU ANALYSIS 303 using user-friendly face morphing software that is either freely available or can be purchased at a reasonable price

In general, the morphing process of face images can be divided into three steps.

First, a correspondence between the contributing samples is determined. In a second step, called warping, both images are distorted, such that the corresponding elements of both samples are geometrically aligned. Finally, the color values of the warped images are merged, referred to as blending, in order to create the morphed face image.

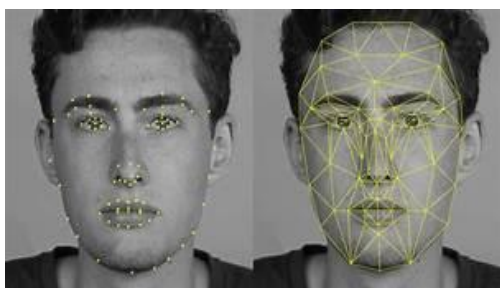
CORRESPONDENCE

The most common way of determining correspondences between face images is by determining salient points in both images, so-called landmarks. The simplest way is to manually define the coordinates of prominent characteristics, e.g.,

eyes, eyebrows, tip of the nose, etc., as for instance done in the morphing process.

WARPING

If the landmarks are determined, the image should be distorted in a manner, that corresponding landmarks are aligned. A straight forward method for morphing is scattered data interpolation [25]. The landmarks, also called control points, are moved to a new position, the new position of all intervening pixels is interpolated based on the nearby control points. More advanced morphing techniques take the correlation between the landmarks into account



BLENDING

After the alignment of the two contributing images, the two arranged textures are combined using blending, usually over the entire image region. The most frequent way of blending for face morph creation is linear blending, i.e. all colour value set same pixel positions are combined in the same manner. Similar to the warping process the contribution to the blending of each image can be weighted by an α -value, e.g. $\alpha = 0.5$ for averaging. The impact of a changing α -value to the morphed image can be seen in on the vertical axis.

This work represents a significant extension of the preliminary studies towards PRNU-based morphing attack detection previously published in [5], [10]. The proposed system has been complemented by a more thorough investigation of different features and aggregation strategies, more specifically spatial features have been investigated in addition to spectral ones from previous work. Complementary to those efforts experiments on morphed face images generated by four different morphing algorithms have been conducted. The generalizability of the PRNU-based morphing attack detection across a wide range of distinct cameras of various makers is further investigated on a database specifically built for PRNU analysis in digital image forensics and it is suitable to determine the decision threshold for the proposed system.

II. RELATED WORKS

In recent years Morphing is an image processing technique used for the metamorphosis from one image to another. The idea is to get a sequence of intermediate images which when put together with the original images would represent the change from one image to the other. The simplest method of transforming one image into another is to cross-dissolve between them. In this method, the colour of each pixel is interpolated over time from the first image value to the corresponding second image value. This is not so effective in suggesting the actual metamorphosis. For morphs between faces, the metamorphosis does not look good if the two faces do not have the same shape approximately. In this project, we implemented a morphing scheme which would combine cross-dissolve with warping methods to give good morphs. This is based on "Feature-Based Image Metamorphosis" by Thaddeus Beier and Shawn Neely. The morph process consists of a warping stage before cross-dissolving so that the two images have the same shape. The warp is specified, in this case, by a mapping between lines in the first and second images. In the following discussion, the first image will be called the source image and the last image will be called the destination image.

In some papers more than one system was presented, in such cases approaches that showed the best performance in detecting morphing attacks are listed. It is important to note that the generalizability/robustness of the published approaches could not be demonstrated. So far, there are no publicly accessible large databases of bona fide and morphed facial images and hardly any publicly available morph recognition algorithms which allow comprehensive experimental evaluations. The vast majority of published methods were trained and tested on various sequestered databases, which hampers reproducibility of results. In addition, morph detection methods are usually trained and tested on a single database with a single morph generation algorithm. Based on these facts, a comparison of published approaches with respect to reported detection performance would be potentially misleading and is deliberately avoided in this work. However, it is expected that planned benchmark tests, e.g., by the National Institute of Standards and Technology (NIST) [40], will enable a meaningful quantitative comparison of published approaches in the near future. Both PRNU-based morph detection approaches analyse the Fourier Spectrum of the PRNU and quantify spectral differences between bona fide and morphed images using statistical measures. The main difference between both approaches lies within the processing pipeline, block-based analysis in the spatial [5], [10]

vs.spectral domain. After that we go for pre processing step. Image fusion for better performance.

III. PROPOSED SYSTEM

This paper gives clear idea about identification of bona fide and morphed images based on decision threshold values using PRNU extraction. This involves five steps pre processing, PRNU cells extraction, spatial feature extraction, spectral features extraction, aggregation, decision threshold. In this first stage we extract face image for particular size(112x92). If the images is in colour then we have to convert in to grey images. After that we go for pre processing step. In this first stage we extract face image for particular size(112x92).

The images is in colour then we have to convert in to grey images. After that we go for pre processing step.

Step 1:

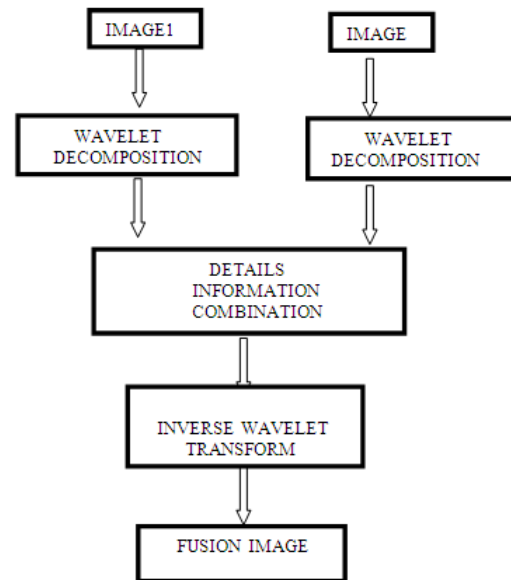
In this first stage we extract face image for particular size(112x92). If the images is in colour then we have to convert in to grey images. After that we go for pre processing step. We pre process image by using image morphing technique called image fusion technique there are other techniques for morphing images we use image fusion for better performance.

Image fusion refers to the techniques that integrate complementary information from multiple image sensor data such that the new images are more suitable for the purpose of human visual perception and computation of processing tasks. Although an increasing number of high resolution images are available along with sensor technology development, image fusion is still a popular and important method to interpret the image data for obtaining a more suitable image for a variety of applications, such as visual interpretation and digital classification.[17] The fused image should have more complete information which is more useful for human or machine perception.

Image fusion is important in many different image processing fields such as satellite imaging, remote sensing and medical imaging.[16] In wavelet fusion method, decomposition of images is done and detail components of decomposition are added at different levels to obtain the new detail components in the different bands of the image which causes merging or fusion of 2 images. The inverse discrete wavelet transform is used to

reconstruct the fused image. The fused image better preserves details and edge of the input or source images. The result of the fused image is excellent.

FIGURE1: FLOW CHART OF IMAGE FUSION ALGORITHM



First step in fusion using wavelet transformation consists in extracting the structures (also called details) present between the images of two different resolutions. These structures are isolated into three wavelet coefficients which correspond to detail images according to three directions (vertical, horizontal and diagonal). In wavelet decomposition four components are calculated from different possible combination of row and column filtering. Adding approximate components of image1 to approximate components of image2, similarly adding detail components of image1 to detail components of image2, we will get approximate and detail components of target image. . Inverse wavelet transform is applied to the fused components to create the fused image. There are hundreds of mother or base wavelets available for decomposition. In practice a mother wavelet is selected from ready-made wavelets for a particular problem and different wavelets $\psi(x)$ have different effects. For instance, Harr wavelets are suitable for the representing a piecewise signal and Daubechies wavelets are more suitable for compressing data. The Daubechies series is the most commonly used series for wavelet decomposition.



Step 2:

PRNU extraction

The PRNU is extracted from the preprocessed image.using the wavelet-based denoising filter can be extracted by using dwt.Discrete Wavelet Transform is the most common form of transform type image fusion algorithm due to its simplicity and ability to preserve time and frequency details of the image to be fused. Similar to Fourier analysis, where sinusoids are chosen as the basis functions, wavelet analysis is based on a decomposition of a signal using an orthonormal family of basis functions. Unlike a sine wave, a wavelet has its energy concentrated in time or space. Sinusoids are useful in analyzing periodic and time invariant phenomenon, while wavelets are well suited for the analysis of transient, time-varying signals. Accordingly, in spatial domain DWT analysis also gives the best performance in detecting discontinuities or subtle changes in gray level. The following essential properties, based on the characteristics of the PRNU described by Fridrich in [19], make the PRNU well suited for a face morph detection scenario:

- 1) Dimensionality: The sensor fingerprint is stochastic in nature and has a large information content, which makes it unique to each sensor.
- 2) Unavoidability: All imaging sensors exhibit PRNU.
- 3) Universality: The sensor fingerprint is present in every picture independently of the camera optics, camera settings, or scene content, with the exception of completely dark images.
- 4) Permanence: It is stable in time and under a wide range of environmental conditions (temperature, humidity, etc.).
- 5) Robustness: It survives lossy compression, filtering, gamma correction, and many other typical processing procedures. It is even reported to survive high quality printing and scanning [18].

In this section, we describe the algorithm for computing the two-dimensional DWT through repeated application of the one-dimensional DWT. The two-dimensional DWT is of particular interest for image processing and computer vision applications, and is a relatively straightforward extension of the one-dimensional DWT discussed above.

$$\text{PRNU noise residual } WI=I-F(I) \text{ -----(1)}$$

I=Morphed image

F(I) =denoising filter function According to fridrich[20]

Below block diagram illustrates the basic, one-level, two-dimensional DWT procedure. First, we apply a one-level, one dimensional DWT along the rows of the image. Second, we apply a one-level, one-dimensional DWT along the columns of the transformed image from the first step. As depicted in Figure (left), the result of these two sets of operations is a transformed image with four distinct bands: (1) LL, (2) LH, (3) HL and (4) HH. Here, L stands for low-pass filtering, and H stands for high-pass filtering. The LL band corresponds roughly to a down-sampled (by a factor of two) version of the original image. The LH band tends to preserve localized horizontal features, while the HL band tends to preserve localized vertical features in the original image. Finally, the HH band tends to isolate localized high-frequency point features in the image. As in the one-dimensional case, we do not necessarily want to stop there, since the one-level, two-dimensional DWT extracts only the highest frequencies in the image. Additional levels of decomposition can extract lower frequency features in the image; these additional levels are applied only to the LL band of the transformed image at the previous level.

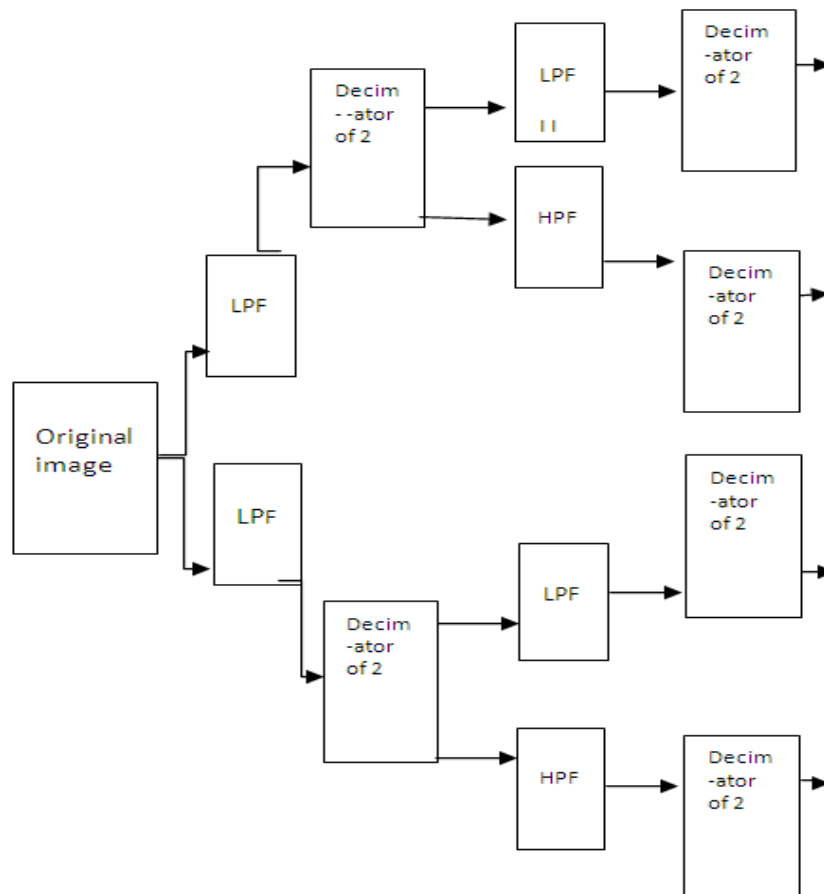
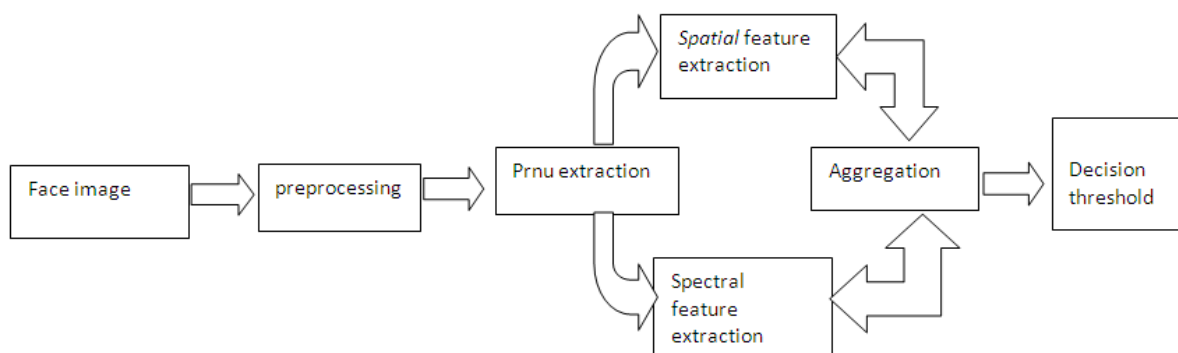


Figure2: BLOCK DIAGRAM OF DWT.

BLOCK DIAGRAM OF PRPOSED METHOD:



Step 3:

The feature extraction is performed individually for each cell. In previous work [5], [10], only spectral features based on the DFT magnitude histogram and magnitude energy have been investigated.

In this work, two different feature types are investigated: spectral features based on the PRNU's DFT magnitudes and new spatial features based on the PRNU values, since the PRNU values are affected by the morphing procedures and post-

processings in the spatial domain as well the spectral one

Both feature types are described in more detail in the following.

Spatial Features: The newly proposed spatial features aim at analysing the distribution of the PRNU values, which is observed to differ between bona fide and morphed images according to Fig. 3(a) and Fig. 3(b). For the first spatial feature, Pvar, the histogram of the PRNU values is computed, which is constrained to a range of [-5, 5] and

divided into 100 bins. These values have been selected by analysing the DFT spectra of extracted PRNUs of bona fide and morphed images. Due to the different slope of bona fide and morphed image's PRNU value distributions that can be observed in we decided to compute the variance of the histogram bin frequencies Pvar, which we defined as

$$Pvar = 1/B \sum_{n=1}^B (Hp(n) - H^-P)^2 \quad (2)$$

where B is the number of bins in the PRNU cell's histogram HP. H⁻ P represents the mean frequency of the histogram bins.

As second spatial feature, we consider the energy of the PRNU values, Pen, which is defined as : Pen = $\sum_{x \in V} |X|$ (3)

where x is a value within all PRNU values V of a cell As the Eqs. (2) and (3) show, both spatial features yield a simple scalar value SV for each PRNU cell.

Spectral Features: In order to compute the spectral features, the first step consists in obtaining the frequency spectrum of the PRNU in each cell, which is done by means of the DFT. The DFT magnitude histograms are constrained to the same universal range of [0, 8] and are divided into 100 bins. These values have again been estimated by analysing the DFT spectra of extracted PRNUs of bona fide and morphed images. Based on the observations in Stage2, we select the variance of the histogram Dvar as being suited for the discrimination between bona fide and morphed images. We obtain Dvar in a similar manner as the previously described Pvar:

$$Dvar = \frac{1}{B} \sum_{n=1}^B (HM(n) - H^-M)^2 \quad (4)$$

where B is the number of bins in a cell's DFT magnitude histogram HM, with H⁻ M being the mean frequency of the histogram bins.

IV. EVALUATION OF PARAMETER

Peak Signal-to-Noise Ratio(PSNR):

Is used to calculate the signal to noise ratio for morphed and bonafide images.

$$PSNR = 10 \log_{10} \left[\frac{K^2}{MSE} \right]$$

V. RESULTS

Below results are the morphed and bonafide images PRNU extraction pattern after that DFT plot for

On the other hand, we propose to compute the energy of the PRNU's DFT magnitudes Den, as defined in Eq. (5), where M are the DFT magnitudes within a cell and x their respective values.

$$Den = \sum_{x \in m} |X|^2 \quad (5)$$

As for the spatial features, both spectral features yield a simple scalar value SV for each PRNU cell when considering Eqs. (4) and (5).

Step 4:

Feature Aggregation

After obtaining the scalar values SV for all cells Cn, the values are aggregated to obtain a global aggregation score A for the image. We investigated various strategies, where we present the two best performing ones. The aggregation calculation formulae written below:

$$Amin = \min SVn \quad (6)$$

$$\forall n \in 1_N$$

$$Amax = \max SVn \quad (6)$$

$$\forall n \in 1_N$$

where N is the number of total cells and SVn is the feature (scalar value) obtained for the cell Cn, as described in the previous processing step. Amin yields the minimum score among the individual cells, while Amax characterizes maximum score among all cells.

Step 5: Descion

Hence, we introduce an additional decision step and derive a mean value B⁻ from bona fide images, where the characteristics of the PRNU are well known. With this property, we can calculate the distance D of an investigated image to bona fide images as

$$D = |A - B^-| \quad (8)$$

$$B^- = 1/NB \sum_{n=1}^{NB} A \quad (9)$$

where A is the cell aggregation result, B⁻ is the mean variation of the NB bona fide images.

Where K represent the maximum possible value of the pixel in an image (e.g:for a gray-scale image the maximum value is 255) and MSE is the mean square error.

spatial feature extraction and also absolute dft plot for spectral feature

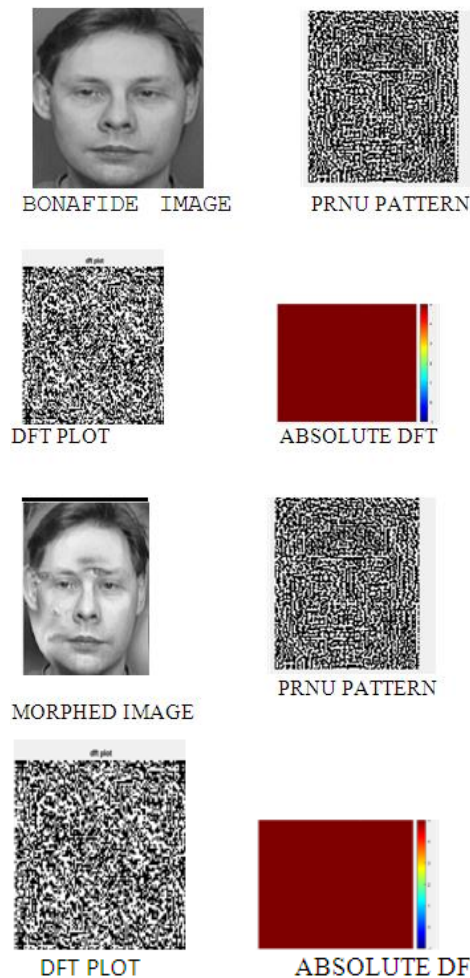


TABLE1: REPRESENTS VALUES FOR VARIANCE, ENERGY

Type of image	Pvar	Pen	Dvar	Den
Morphed images	3.1302e+03	3.4021e+03	1.9740e+03	3.4050e+03
Bonafide images	3.1304e+03	3.4983e+03	1.9740e+03	3.4829e+03

TABLE2: REPRESENTS VALUES FOR PSNR

Type of image	psnr
Morphed images	40.1294
Bonafide images	41.8607

TABLE 3 : DECISION VALUES FOR BONAFIDE AND MORPHED IMAGES.

TYPE OF IMAGE	DECISION THRESHOLD VALUES			
BONAFIDE IMAGES	0.9847	0.5596	0.9043	0.5514
MORPHED IMAGES	0.489	0.3211	0.2122	0.4321

It has to be noted that based features Pen and Den, while it is not calculated for the features of Pvar and Dvar, due to dft plot yielding more consistent scores among different post processings which can be classified with a one dimensional threshold.

If the distance calculation is applied, the final decision for a presented face image is taken by thresholding the calculated distance D. Otherwise, the final decision simply relies on thresholding of the value A, which is obtained directly from the cell aggregation.

VI. CONCLUSION

As we have observed in table 2 if all the decision threshold values are less than 0.5 then the given image is said to be morphed image. If all the decision threshold values are nearly equal to 1 then the image is said to be bonafide image.

We have taken decision threshold because as compared to previous works they have done only preprocessing techniques but we have calculated main parameter PRNU from that we are extracting spatial and spectral feature so our model gets more accuracy Of 86%.

REFERENCES

- [1]. W. Zhao, R. Chellappa, P. J. Phillips, and A. Rosenfeld, "Face recognition: A literature survey," ACM Comput. Surv., vol. 35, no. 4, pp. 399–458, Dec. 2003.
- [2]. S. Z. Li and A. K. Jain, Eds., Handbook of Face Recognition. London, U.K.: Springer, 2011
- [3]. F. Schroff, D. Kalenichenko, and J. Philbin, "FaceNet: A unified embedding for face recognition and clustering," in Proc. IEEE Conf. Comput. Vis. Pattern Recognit. (CVPR), Jun. 2015, pp. 815–823.
- [4]. O. M. Parkhi, A. Vedaldi, and A. Zisserman, "Deep face recognition," in Proc. Brit. Mach. Vis. Conf. (BMVC), 2015, p. 6.
- [5]. M. Ferrara, A. Franco, and D. Maltoni, "The magic passport," in Proc. IEEE Int. Joint Conf. Biometrics (IJCB), Sep./Oct. 2014, pp. 1–7.
- [6]. U. Scherhag, C. Rathgeb, J. Merkle, R. Breithaupt, and C. Busch, "Face recognition systems under morphing attacks: A survey," IEEE Access, vol. 7, pp. 23012–23026, 2019.
- [7]. G. Wolberg, "Image morphing: A survey," Vis. Comput., vol. 14, nos. 8–9, pp. 360–372, Dec. 1998.

- [8]. A. Patel and P. Lapsiwala, "Image morphing algorithm: A survey," *Int. J. Comput. Appl. (IJCA)*, vol. 5, no. 3, pp. 156–160, 2015.
- [9]. U. Scherhag, C. Rathgeb, and C. Busch, "Towards detection of morphed face images in electronic travel documents," in *Proc. 13th IAPR Workshop Document Anal. Syst. (DAS)*, 2018, pp. 187–192.
- [10]. M. Ferrara, A. Franco, and D. Maltoni, "On the effects of image alterations on face recognition accuracy," in *Face Recognition Across the Imaging Spectrum*. Cham, Switzerland: Springer Int., 2016, pp. 195–222.
- [11]. D. J. Robertson, A. Mungall, D. G. Watson, K. A. Wade, S. J. Nightingale, and S. Butler, "Detecting morphed passport photos: A training and individual differences approach," *Cogn. Res. Princ. Implicat.*, vol. 3, no. 1, p. 27, Jun. 2018.
- [12]. D. Ruprecht and H. Muller, "Image warping with scattered data interpolation," *IEEE Comput. Gra*
- [13]. M. Ngan, P. Grother, and K. Hanaoka, "Performance of automated facial morph detection and morph resistant face recognition algorithms,
- [14]. L. Debiasi, U. Scherhag, C. Rathgeb, A. Uhl, and C. Busch, "PRNUbased detection of morphed face images," in *Proc. IEEE 6th Int. Workshop Biometrics Forensics (IWBF)*, 2018, pp. 1–7.
- [15]. L. Debiasi, C. Rathgeb, U. Scherhag, A. Uhl, and C. Busch, "PRNU variance analysis for morphed face image detection," in *Proc. 9th IEEE Int. Conf. Biometr. Theory Appl. Syst. (BTAS)*, 2018, pp. 1–9.
- [16]. L.-B. Zhang, F. Peng, and M. Long, "Face morphing detection using Fourier spectrum of sensor pattern noise," in *Proc. IEEE Int. Conf. Multimedia Expo (ICME)*, Jul. 2018, pp. 1–6.
- [17]. H. Li, B.S. Manjunath, and S.K. Mitra, *Multisensor Image Fusion Using Wavelet Graphical Models And Image Processing*
- [18]. *Wavelets For Image Fusion*, Stavri Nikolov, Paul Hill, David Bull, Nishan Canagarajah, Image Processing Group.
- [19]. J. Fridrich, "Sensor defects in digital image forensics," in *Digital Image Forensics: There Is More to a Picture Than Meets the Eye*, H. Sencar and N. Memon, Eds. New York, NY, USA: Springer-Verlag, 2012, ch. 6. [81] M. Goljan, J. Fridrich, and J. Lukas, "Camera identification from printed images," in *Proc. SPIE Electron. Imag. Forensics Security Steganography Watermarking Multimedia Contents X*, 2008, Art. no. 68190I.
- [20]. J. Lukáš, J. Fridrich, and M. Goljan, "Digital camera identification from sensor pattern noise," *IEEE Trans. Inf. Forensics Security*, vol. 1, no. 2, pp. 205–214, Jun. 2006. [83] T. Gloe, M. Kirchner, A. Winkler, and R. Böhme, "Can we trust digital image forensics?" in *Proc. 15th ACM Int. Conf. Multimedia*, 2007,
- [21]. J. Fridrich, "Digital image forensic using sensor noise," *IEEE Signal Process. Mag.*, vol. 26, no. 2, pp. 26–37, Mar. 2009
- [22]. U. Scherhag, C. Rathgeb, and C. Busch, "Morph detection from single face image: A multi-algorithm fusion approach," in *Proc. Int. Conf. Biometr. Eng. Appl. (ICBEA)*, 2018, pp. 6–12.
- [23]. P. J. Phillips, H. Wechsler, J. Huang, and P. J. Rauss, "The FERET database and evaluation procedure for face-recognition algorithms," *Image Vis. Comput.*, vol. 16, no. 5, pp. 295–306, Apr. 1998.
- [24]. A. Martinez and R. Benavente, "The AR face database," *Comput. Vis. Center, Universitat Autònoma de Barcelona, Barcelona, Spain, Rep. 24*, Jun. 1998.
- [25]. L. Spreeuwers, M. Schils, and R. Veldhuis, "Towards robust evaluation of face morphing detection," in *Proc. 26th Eur. Signal Process. Conf. (EUSIPCO)*, 2018, pp. 1027–1031
- [26]. N. Damer, A. M. Saladie, A. Braun, and A. Kuijper, "MorGAN: Recognition vulnerability and attack detectability of face morphing attacks created by generative adversarial network," in *Proc. 9th IEEE Int. Conf. Biometr. Theory Appl. Syst. (BTAS)*, 2018, pp. 1–10.
- [27]. Z. Liu, P. Luo, X. Wang, and X. Tang, "Deep learning face attributes in the wild," in *Proc. IEEE Int. Conf. Comput. Vis. (ICCV)*, Dec. 2015, pp. 3730–3738.
- [28]. L.-B. Zhang, F. Peng, and M. Long, "Face morphing detection using Fourier spectrum of sensor pattern noise," in *Proc. IEEE Int. Conf. Multimedia Expo (ICME)*, Jul. 2018, pp. 1–6.
- [29]. C. E. Thomaz and G. A. Giralardi, "A new ranking method for principal components analysis and its application to face image analysis," *Image Vis. Comput.*, vol. 28, no. 6, pp. 902–913, Jun. 2010.
- [30]. M. Hildebrandt, T. Neubert, A. Makrushin, and J. Dittmann, "Benchmarking face morphing forgery detection: Application of stirtrace for impact simulation of different processing steps," in *Proc. IEEE 5th Int.*

- Workshop Biometr. Forensics (IWBF), Apr. 2017, pp. 1–6.
- [31]. C. Seibold, A. Hilsmann, and P. Eisert, “Reflection analysis for face morphing attack detection,” in Proc. 26th Eur. Signal Process. Conf. (EUSIPCO), 2018, pp. 1022–1026.
- [32]. R. Ramachandra, S. Venkatesh, K. Raja, and C. Busch, “Detecting face morphing attacks with collaborative representation of steerable features,” in Proc. 3rd Comput. Vis. Image Process. (CVIP), 2018, pp. 1–11.
- [33]. R. Ramachandra, K. B. Raja, S. Venkatesh, and C. Busch, “Transferable deep-CNN features for detecting digital and print-scanned morphed face images,” in Proc. IEEE Conf. Comput. Vis. Pattern Recognit. Workshops (CVPRW), Jul. 2017, pp. 1822–1830.
- [34]. C. Seibold, W. Samek, A. Hilsmann, and P. Eisert, “Accurate and robust neural networks for security related applications exemplified by face morphing attacks,” in Proc. Comput. Vis. Pattern Recognit. (CVPR), 2018, pp. 1–16.
- [35]. L. Yin, X. Wei, Y. Sun, J. Wang, and M. Rosato, “A 3D facial expression database for facial behavior research,” in Proc. IEEE 7th Int. Conf. Autom. Face Gesture Recognit. (FGR), 2006, pp. 211–216.
- [36]. D. S. Ma, J. Correll, and B. Wittenbrink, “The chicago face database: A free stimulus set of faces and norming data,” *Behav. Res. Methods*, vol. 47, no. 4, pp. 1122–1135, Jan. 2015